Cellular Microbiology (2008) **10**(2), 499–513

doi:10.1111/j.1462-5822.2007.01065.x
First published online 2 November 2007

# A C-terminal class I PDZ binding motif of EspI/NleA modulates the virulence of attaching and effacing *Escherichia coli* and *Citrobacter rodentium*

**Sau Fung Lee,[1] Michelle Kelly,[1] Adrian McAlister,[1] Shelley N. Luck,[1] Erin L. Garcia,[2] Randy A. Hall,[2] Roy M. Robins-Browne,[3,4] Gad Frankel[5] and Elizabeth L. Hartland[1,3,4]***

[1]*Department of Microbiology, Monash University, Clayton, Victoria 3800, Australia.*
[2]*Department of Pharmacology, Emory University School of Medicine, Atlanta, GA 30322, USA.*
[3]*Department of Microbiology and Immunology, University of Melbourne, Victoria 3010, Australia.*
[4]*Murdoch Children's Research Institute, Royal Children's Hospital, Parkville, Victoria 3052, Australia.*
[5]*Division of Cell and Molecular Biology, Imperial College London, London SW7 2AZ, UK.*

## Summary

**Enteropathogenic *Escherichia coli* induces characteristic attaching–effacing (A/E) lesions on the intestinal mucosa during infection. The locus of enterocyte effacement is essential for A/E lesion formation and encodes a type III secretion system that translocates multiple effector proteins into the host cell. Following translocation, EspI/NleA localizes to the Golgi. Using the yeast two-hybrid system (Y2HS) and PSD-95/Disk-large/ZO-1 (PDZ)-domain protein array overlays, we identified 15 putative host-interacting partners of EspI. All but two of the target proteins contained PDZ domains. Examination of the EspI amino acid sequence revealed a C-terminal consensus class I PDZ binding motif. Deletion of the last 7 amino acids of EspI to generate $EspI_{\Delta C7}$ abrogated the Y2HS interaction between EspI and 5 of the 6 putative host cell target proteins tested. Deletion of the EspI PDZ binding motif also resulted in delayed trafficking of EspI to the Golgi. Using a mouse model of infection, we showed that *Citrobacter rodentium* expressing truncated $EspI_{\Delta C7}$ was attenuated when in competition with *C. rodentium* expressing full-length EspI. Overall, these results suggested that EspI may modulate the virulence of A/E pathogens by binding host PDZ-domain proteins.**

Received 6 February, 2007; revised 20 August, 2007; accepted 19 September, 2007. *For correspondence. E-mail hartland@unimelb.edu.au; Tel. (+61) 3 8344 8041; Fax (+61) 9347 1540.



## Introduction

Enteropathogenic *Escherichia coli* (EPEC) is an important human pathogen that causes severe diarrhoea in young children. A feature of EPEC colonization is the formation of attaching–effacing (A/E) lesions on the host gastrointestinal tract during infection. EPEC is a member of a group of A/E pathogens that carry the locus of enterocyte effacement (LEE) pathogenicity island that is required for A/E lesion formation (Elliott *et al*., 1998). The LEE encodes transcriptional regulators, the adhesin, intimin (Jerse *et al*., 1990), a type III secretion system (T3SS) (Jarvis and Kaper, 1996), translocators, chaperones and effector proteins that are translocated by the T3SS into the eukaryotic cell (Garmendia *et al*., 2005). A/E lesions are characterized by localized effacement of the brush-border microvilli, intimate attachment of the bacteria to the host cell plasma membrane, and the subsequent formation of actin-rich pedestal-like structures adjacent to adherent bacteria (Garmendia *et al*., 2005). Because EPEC is a human-specific pathogen, infection of mice with the A/E pathogen, *Citrobacter rodentium*, is commonly used as a model for EPEC infection (reviewed in Mundy *et al*., 2005). *C. rodentium* induces A/E lesions in mice that are indistinguishable from those caused by other A/E pathogens (Schauer and Falkow, 1993).

Although EPEC and other A/E pathogens generally remain extracellular and attached to the apical surface of enterocytes, all A/E pathogens are able to interfere with internal host cell processes through the LEE T3SS-dependent translocation of multiple effector proteins (Tobe *et al*., 2006). A minority of these effectors are encoded by genes within the LEE (Tobe *et al*., 2006). One of the LEE-encoded effector proteins, Tir (Kenny *et al*., 1997), is integrated into the host cell plasma membrane, where it adopts a hairpin loop topology (Hartland *et al*., 1999). Through the central extracellular domain, Tir acts as a receptor for intimin (Hartland *et al*., 1999; Kenny, 1999). This specific interaction between intimin and Tir is central to intimate attachment of bacteria to the host epithelium (Batchelor *et al*., 2000; Luo *et al*., 2000).

Simultaneously, through the intracellular amino and carboxy termini, Tir interacts with several cytoskeletal proteins, linking the extracellular bacterium to the host cell cytoskeleton (Goosney *et al*., 2000; Gruenheid *et al*., 2001; Batchelor *et al*., 2004).

EspI (also termed NleA) is a non-LEE-encoded effector protein that is not required for A/E lesion formation but contributes to bacterial colonization and the induction of hyperplasia in the colonic epithelium of mice infected with *C. rodentium* (Gruenheid *et al*., 2004; Mundy *et al*., 2004a). In EPEC and the human pathogen enterohaemorrhagic *E. coli* (EHEC), the gene encoding EspI is more frequent among strains associated with severe disease, suggesting that the protein also has an important role in virulence in these pathogens (Mundy *et al*., 2004b). Following translocation, EspI is rapidly targeted to the Golgi apparatus of eukaryotic cells, where it colocalizes with mannosidase II and Golgin-97 (Gruenheid *et al*., 2004; Creuzburg *et al*., 2005), but it is not known whether this trafficking event is important or relevant to the function of EspI. EspI does not contain classical Golgi-targeting motifs and may be targeted to the Golgi apparatus via novel Golgi-targeting motifs or by interaction with other Golgi-associated host cell proteins (Gruenheid *et al*., 2004).

Although *espI* contributes to the virulence of *C. rodentium* and was identified twice in *C. rodentium* signature-tagged mutagenesis screens (Mundy *et al*., 2004a; Kelly *et al*., 2006), the host target of this protein and its mechanism of action are unknown. To elucidate the role of EspI in the host–pathogen interaction, we used the yeast two-hybrid system (Y2HS) to identify potential host cell binding partners that may be affected by EspI function. The Y2HS screen of a HeLa cell cDNA library yielded six putative interacting host proteins, four of which contained reported PSD-95/Disk-large/ZO-1 (PDZ) domains. PDZ domains are common protein–protein interaction domains in eukaryotic proteins that are present in up to 0.5% of open reading frames. Typically PDZ-domain proteins are involved in the assembly of host cell multiprotein signalling complexes (Harris and Lim, 2001). A PDZ-domain comprises ~90 amino acids that form a series of six β-strands and two α-helices that fold into a six-stranded β-sandwich (Jelen *et al*., 2003; Piserchio *et al*., 2006). PDZ domains recognize a C-terminal amino acid motif on target proteins comprising a ~5-amino-acid core recognition motif that serves as an additional antiparallel β-strand during a PDZ domain–ligand interaction (Jelen *et al*., 2003; Piserchio *et al*., 2006; Zhang *et al*., 2006). PDZ domains may be classified according to the C-terminal peptide they recognize. Class I PDZ domains recognize the consensus amino acid sequence x-[S/T]-x-[V/L/I]-$_{COOH}$, class II PDZ domains recognize Φ-x-Φ-$_{COOH}$, and class 3 PDZ domains recognize a target sequence x-x-$C_{COOH}$, where x is any amino acid and Φ is a hydrophobic amino acid (Songyang *et al*., 1997; Harris and Lim, 2001; Jelen *et al*., 2003). Residues at positions 0 and −2 (where the C-terminal amino acid is position 0) are critical for binding, but the specificity and affinity of binding may be greatly influenced by upstream amino acids (Piserchio *et al*., 2006; Zhang *et al*., 2006). For example, amino acids up to −10 have been reported to participate in PDZ interactions (Lim *et al*., 2002). Therefore, the specificity and affinity of PDZ interactions can vary considerably. While some PDZ domain–ligand interactions are highly specific, others are quite promiscuous (Lim *et al*., 2002; Zhang *et al*., 2006). In this study, we found that EspI contained a class I consensus PDZ binding motif at the C-terminus, which was highly conserved among A/E pathogens. Here we examined the contribution of the PDZ binding ligand of EspI to host protein interactions, to Golgi trafficking and to the virulence of *C. rodentium*.

## Results

### *Identification of putative host cell-interacting partners of EspI*

To identify potential eukaryotic interacting partners of EspI, we performed a Y2HS screen of a pretransformed HeLa cDNA library using the full-length EspI from EPEC E2348/69 as bait. Thirty-two yeast colonies were obtained from the library screen following growth of the diploids on medium that selects for protein–protein interactions. Sequencing of rescued cDNA plasmids from positive yeast colonies yielded six different putative host cell-interacting partners of EspI. Five of the six targets were identified multiple times, with eight independent hits for Sec24B and PDZK11 (Table 1). Four of the six putative EspI-interacting proteins contained PDZ domains (Table 1). Expression of the Y2HS reporter, *lacZ*, was assayed by measuring β-galactosidase activity in yeast clones carrying the bait and prey plasmids to assess the relative affinity of EspI binding to the various putative host cell targets. Yeast strains expressing EspI and the respective HeLa proteins showed a 5- to 40-fold increase in β-galactosidase activity compared with the negative control yeast strains, thereby confirming a genuine interaction of EspI with all six proteins in the Y2HS (Fig. 1A).

Although the Y2HS is a powerful screening tool to detect protein interactions, it has an inherent limitation as some interactions are not permissive in yeast, thus producing false-negative results. Given the observation that EspI interacted with several host cell proteins containing PDZ domains, we hypothesized that EspI may recognize additional host PDZ-domain proteins. In order to address this experimentally, we fused the last 50 amino acids of EspI to glutathione S-transferase (GST) and screened a

**Table 1.** Eukaryotic EspI binding proteins identified from Y2HS screen of a HeLa cDNA library.

| EspI binding protein | GenBank accession number | Number of times identified | Predicted Pfam domains[a] | Total amino acids | Amino acids (and domains) in Y2HS clone | Function |
|---|---|---|---|---|---|---|
| α1 syntrophin | AAB36398 | 6 | PDZ, PH, SU | 505 | 79–300 (PDZ, PH) | Targeting of signalling proteins and maintaining membrane integrity |
| MALS3 | BAD96876 | 5 | PDZ, L27 | 197 | 1–194 (PDZ, L27) | Protein targeting and trafficking |
| PDZK11 | AAH89433 | 8 | PDZ | 139 | 1–139 (PDZ) | Unknown |
| SNX27 | EAW53427 | 1 | PDZ, PX | 508 | 56–167 (PDZ) | Endocytosis and vesicle trafficking |
| Sec24B | EAX06241 | 8 | Sec23/24 | 1218 | 67–292 | Protein trafficking from ER to the Golgi |
| TCOF1 | EAW61733 | 4 | LisH | 795 | 356–513 | Associated with Treacher Collins–Franceschetti syndrome |

**a.** SU, syntrophin unique; L27, domain found in receptor targeting proteins Lin-2 and Lin-7; PX, phosphoinositide binding domain; Sec23/24, Sec23/24 helical domain; LisH, Lissencephaly type-1-like homology motif.

PDZ-domain protein array for interacting partners. GST–$EspI_{50}$ bound 13 of 96 possible PDZ domains, including 4 isoforms of syntrophin and 2 isoforms of NHERF (Fig. 1B and C, Table 2). In general, the intensity of labelling on the PDZ array corresponds to the strength of the interaction. Thus, it appeared that EspI interactions with the syntrophins, MAGI-3 and PSD-95 were the strongest interactions observed on the array (Fig. 1B). Interestingly, the EPEC effector protein Map was also recently found to bind PDZ1 of NHERF1 via the carboxy-terminal DTRL PDZ binding motif (Alto *et al.*, 2006; Simpson *et al.*, 2006). Overall, we found that EspI had the potential to bind at least 15 host cell proteins.

### *Contribution of a putative C-terminal PDZ binding motif of EspI to protein–protein interactions*

Because four of the six putative host cell binding partners of EspI contained PDZ domains, we examined the amino acid sequence of EspI for a C-terminal PDZ binding motif.

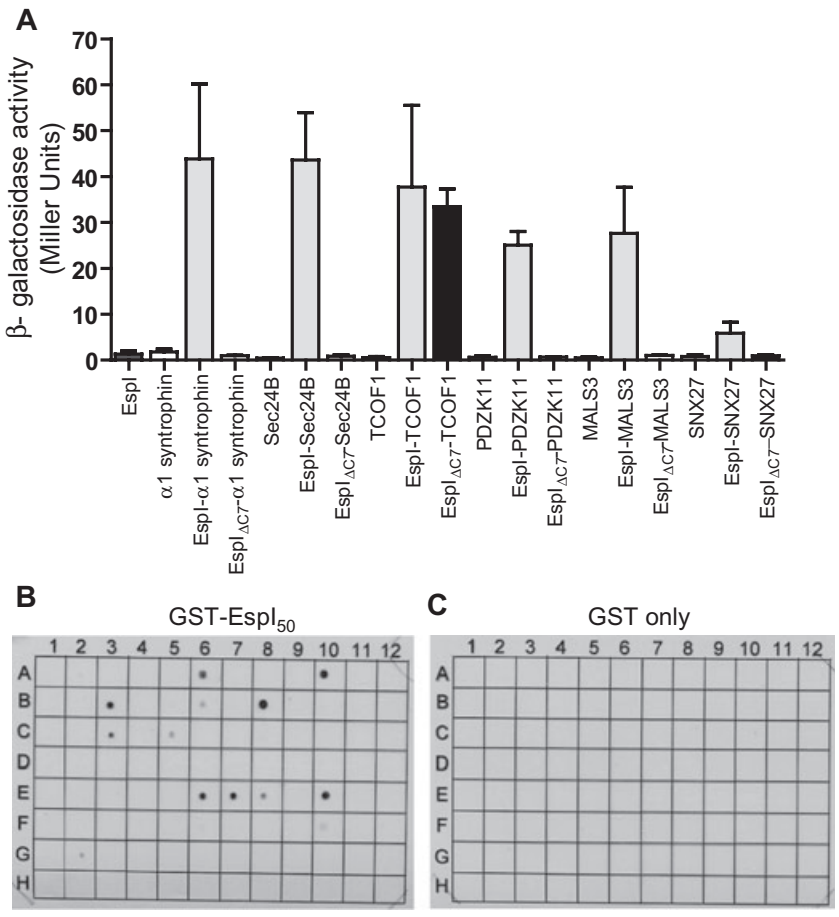


**Fig. 1.** A. Interaction of EspI and EspI$_{\Delta C7}$ from EPEC E2348/69 with α1 syntrophin, Sec24B, TCOF1, PDZK11, MALS3 and SNX27 in the Y2HS. Interactions were analysed by assessing β-galactosidase activity in *S. cerevisiae* strains carrying EspI and EspI$_{\Delta C7}$ fusions to the binding domain of GAL4 and HeLa cDNA fusions to the activation domain of GAL4 as indicated. Results are presented as mean ± standard deviation of at least three biological replicates.
B. PDZ-domain protein array overlaid with purified GST–$EspI_{50}$ and detected with anti-GST antibodies.
C. PDZ-domain protein array overlaid with purified GST and detected with anti-GST antibodies. PDZ domains included on the array are listed in Table 2.

 

**Table 2.** PDZ domains included on protein array.

| Position | PDZ domain[a] | Position | PDZ domain | Position | PDZ domain | Position | PDZ domain |
|---|---|---|---|---|---|---|---|
| A1 | MAGI-1 PDZ1 | C1 | INADL PDZ6 | E1 | RHOPHILIN-2 | G1 | PDZK1 DZ4 |
| A2 | MAGI-1 PDZ2 | C2 | AP97 PDZ1 + 2 | E2 | HARMONIN PDZ1 | G2 | PDZK2 PDZ1[b] |
| A3 | MAGI-1 PDZ3 | C3 | SAP97 PDZ3[b] | E3 | HARMONIN PDZ2 | G3 | PDZK2 PDZ2 |
| A4 | MAGI-1 PDZ4 + 5 | C4 | SAP102 PDZ1 + 2 | E4 | NEURABIN PDZ | G4 | PDZK2 PDZ3 |
| A5 | MAGI-2 PDZ1 | C5 | SAP102 PDZ3[b] | E5 | SPINOPHILIN PDZ | G5 | PDZK2 PDZ4 |
| A6 | MAGI-2 PDZ2[b] | C6 | CHAP110 PDZ1 + 2 | E6 | α1 SYNTROPHIN[b] | G6 | LNX1 PDZ1 |
| A7 | MAGI-2 PDZ3 | C7 | CHAP110 PDZ3 | E7 | β1 SYNTROPHIN[b] | G7 | LNX1 PDZ2 |
| A8 | MAGI-2 PDZ4 | C8 | E6TP1 PDZ | E8 | β2 SYNTROPHIN[b] | G8 | LNX1 PDZ3 |
| A9 | MAGI-2 PDZ5 | C9 | ERBIN PDZ | E9 | γ1 SYNTROPHIN | G9 | LNX1 PDZ4 |
| A10 | MAGI-3 PDZ1[b] | C10 | ZO-1 PDZ1 | E10 | γ2 SYNTROPHIN[b] | G10 | LNX2 PDZ1 |
| A11 | MAGI-3 PDZ2 | C11 | ZO-1 PDZ2 | E11 | PAPIN 1 | G11 | LNX2 PDZ2 |
| A12 | MAGI-3 PDZ3 | C12 | ZO-1 PDZ3 | E12 | MUPP1 PDZ1 | G12 | LNX2 PDZ4 |
| B1 | MAGI-3 PDZ4 | D1 | ZO-2 PDZ1 | F1 | MUPP1 PDZ6 | H1 | PTPN4 PDZ |
| B2 | MAGI-3 PDZ5 | D2 | ZO-2 PDZ2 | F2 | MUPP1 PDZ7 | H2 | RHO-GEF PDZ |
| B3 | NHERF1 PDZ1[b] | D3 | ZO-2 PDZ3 | F3 | MUPP1 PDZ8 | H3 | RA-GEF PDZ |
| B4 | NHERF1 PDZ2 | D4 | ZO-3 PDZ1 | F4 | MUPP1 PDZ10 | H4 | ENIGMA PDZ |
| B5 | HERF2 PDZ1 | D5 | ZO-3 PDZ2 | F5 | MUPP1 PDZ12 | H5 | LARG PDZ |
| B6 | NHERF2 PDZ2[b] | D6 | ZO-3 PDZ3 | F6 | MUPP1 PDZ13 | H6 | MAST205 PDZ |
| B7 | SD-95 PDZ1 + 2 | D7 | C2PA PDZ | F7 | PTPN13 PDZ1 | H7 | PTPN3 PDZ |
| B8 | PSD-95 PDZ3[b] | D8 | GIPC PDZ | F8 | PTPN13 PDZ3 | H8 | SHANK1 PDZ |
| B9 | PDZ-GEF1 PDZ | D9 | MALS1 PDZ | F9 | PTPN13 PDZ4 + 5 | H9 | TAMALIN PDZ |
| B10 | CAL PDZ | D10 | MALS3 PDZ | F10 | PDZK1 PDZ1[b] | H10 | PAR-3 PDZ1 |
| B11 | nNOS PDZ | D11 | DENSIN-180 | F11 | PDZK1 PDZ2 | H11 | PAR-3 PDZ2 |
| B12 | INADL PDZ5 | D12 | RHOPHILIN-1 | F12 | PDZK1 PDZ3 | H12 | PAR-3 PDZ3 |

**a.** Full details of protein domains shown elsewhere (Fam *et al.*, 2005; He *et al.*, 2006).
**b.** Positive interaction with GST–$EspI_{50}$.

Alignment of the amino acid sequences of all EspI proteins available from public databases revealed a consensus class I PDZ binding motif, ETRV, which was conserved among all A/E pathogens. In fact, the C-terminal 7 amino acids were highly conserved among the 18 EspI sequences examined (data not shown). Because up to 10 amino acids of a PDZ ligand may contribute to the PDZ interaction (Lim *et al.*, 2002), we deleted the conserved C-terminal 7 amino acids to determine whether the putative PDZ binding motif played a direct role in EspI–host protein interactions. The truncated protein from EPEC EspI was termed $EspI_{\Delta C7}$. $EspI_{\Delta C7}$ was introduced into the Y2HS and tested against the six host proteins identified by screening with full-length EspI. β-Galactosidase assays showed that upon deletion of the C-terminal 7 amino acids, the interactions between EspI and five of the six host cell proteins were lost. The only interaction to be maintained using $EspI_{\Delta C7}$ was with TCOF1, which does not have a PDZ domain. Interestingly, although Sec24B does not have a reported PDZ domain, EspI interacted with this target in a PDZ motif-dependent manner (Fig. 1A).

In order to determine the specificity of the EspI PDZ binding motif, the 4 C-terminal amino acids of EspI (ETRV) were replaced with the PDZ binding motif of Map (DTRL). $EspI_{DTRL}$ was introduced into the Y2HS and tested for its ability to interact with the six putative Y2HS binding partners of EspI. While interactions with TCOF1 (which binds EspI independently of the ETRV motif) and Sorting Nexin 27 (SNX27) were retained in the Y2HS, $EspI_{DTRL}$ did not support interactions with α1 syntrophin, Sec24B, Mammalian LIN Seven 3 (MALS3) and PDZK11 (Fig. 2).

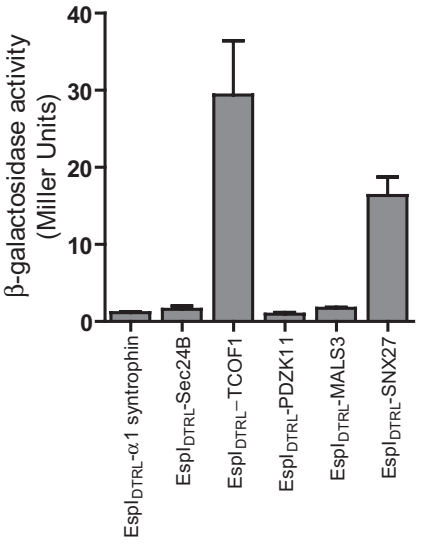


**Fig. 2.** Interaction of $EspI_{DTRL}$ with α1 syntrophin, Sec24B, TCOF1, PDZK11, MALS3 and SNX27 in the Y2HS. Interactions were analysed by assessing β-galactosidase activity in *S. cerevisiae* strains carrying $EspI_{DTRL}$ fusions to the binding domain of GAL4 and HeLa cDNA fusions to the activation domain of GAL4 as indicated. Results are presented as mean ± standard deviation of at least three biological replicates.

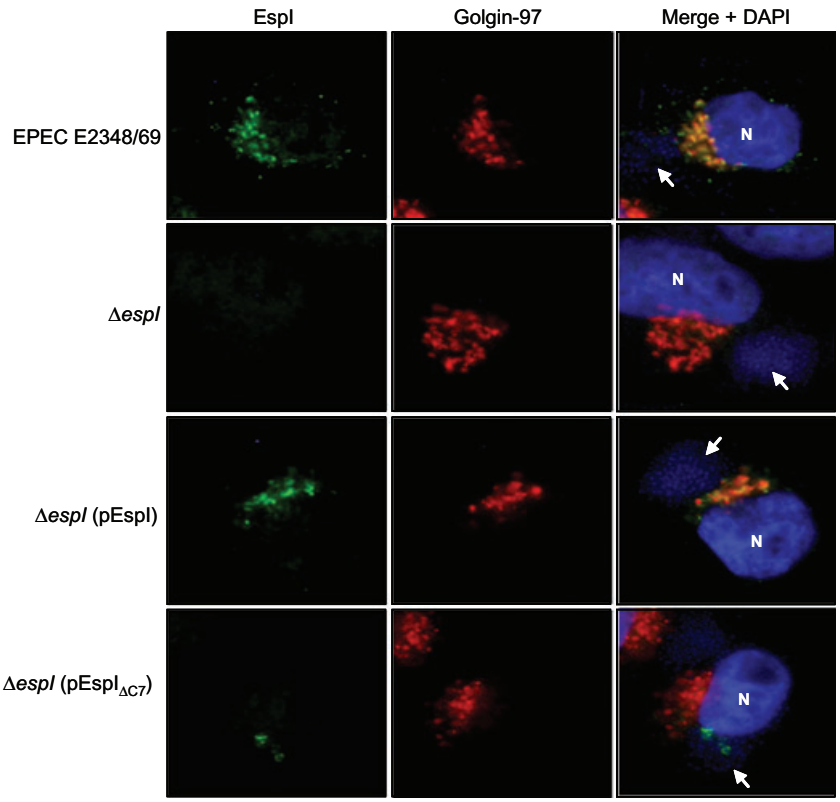


**Fig. 3.** Immunofluorescence microscopy of HeLa cells infected with derivatives of EPEC E2348/69 for 5 h. Cells were stained for EspI (green), Golgin-97 (red), and bacterial and host cell nucleic acid (blue). Arrows indicate bacterial microcolonies, and N signifies HeLa cell nuclei.

*The PDZ binding motif of EspI is important for rapid targeting to the Golgi apparatus*

Previous work has shown that EspI localizes to the Golgi apparatus in infected cells (Gruenheid *et al*., 2004; Creuzburg *et al*., 2005). To determine whether deletion of the C-terminal PDZ binding motif of EspI affected trafficking of the protein to the Golgi, HeLa cells were infected for 5 h with EPEC wild type, EPEC Δ*espI* and EPEC Δ*espI* complemented with full-length *espI* or *espI*$_{\Delta C7}$. As reported previously (Gruenheid *et al*., 2004; Creuzburg *et al*., 2005), immunofluorescence of HeLa cells infected with wild-type EPEC using anti-EspI antibodies resulted in a perinuclear staining pattern typical of Golgi localization, which was absent in cells infected with the Δ*espI* mutant (Fig. 3). EspI staining colocalized extensively with staining for the *trans*-Golgi network resident protein, Golgin-97 (Fig. 3), and was also present periodically at the site of bacterial attachment. Transcomplementation of the Δ*espI* mutant with full-length *espI* restored perinuclear staining but also resulted in increased staining at the bacterial attachment site. In contrast, infection of HeLa cells for 5 h with the Δ*espI* mutant complemented with *espI*$_{\Delta C7}$ resulted in EspI$_{\Delta C7}$ staining almost exclusively at the site of bacterial attachment, which was distinct from the perinuclear staining pattern observed for full-length EspI (Fig. 3). To determine whether trafficking of EspI$_{\Delta C7}$ to the Golgi was prevented or just delayed, we infected HeLa cells for 5 h, after which the bacteria were killed by the addition of penicillin and streptomycin. HeLa cells were then incubated for up to 24 h before fixation and staining for EspI and Golgin-97. At 5, 9, 11 and 24 h after infection, we calculated the percentage of HeLa cells showing EspI Golgi localization for up to 100 HeLa cells that were positive for EspI staining (Fig. 4). At 5, 9 and 11 h, transcomplementation of the *espI* mutant with full-length *espI* resulted in ~25% of HeLa cells showing EspI Golgi localization (Fig. 4). In contrast, at 5 h EspI$_{\Delta C7}$ showed little or no Golgi localization compared with EspI ($P = 0.0014$, unpaired two-tailed *t*-test) (Fig. 4). However, by 11 h EspI$_{\Delta C7}$ Golgi localization was evident and, thereafter, there was no significant difference in Golgi trafficking of EspI and EspI$_{\Delta C7}$. Together these results suggested that the PDZ binding motif of EspI was important for rapid Golgi localization, and that the deletion of the C-terminal 7 amino acids delayed, but did not prevent, EspI–Golgi trafficking. Interestingly by 24 h, even when the Golgi appeared intact, EspI and EspI$_{\Delta C7}$ Golgi localization was no longer apparent, even for HeLa cells infected with wild-type EPEC E2348/69, although some EspI staining was evident at the bacterial attachment site (data not shown). This suggested that EspI Golgi localization was a transient event.

To ensure that the differences in trafficking of EspI and EspI$_{\Delta C7}$ were not due to protein instability or

 

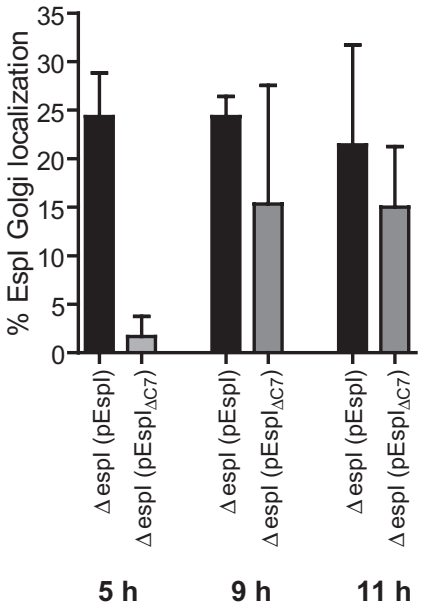


**Fig. 4.** Quantification of EspI Golgi localization in HeLa cells infected with Δ*espI* (pEspI) and Δ*espI* (pEspI$_{\Delta C7}$). HeLa cells were infected for 5 h, after which cells were fixed and stained for EspI and Golgin-97, or bacteria were killed by the addition of penicillin and streptomycin. Following antibiotic treatment, incubation of live cells was continued up to a total of 9 or 11 h, after which the cells were fixed and stained for EspI and Golgin-97. EspI staining from at least 50 cells was scored blind according to the staining pattern shown in Fig. 3. Results are presented as mean ± standard deviation of at least three independent repeats.

translocation inefficiency, we assessed the production and secretion of EspI and EspI$_{\Delta C7}$ by immunoblot. When expressed from pACYC184, both EspI and EspI$_{\Delta C7}$ were secreted in similar amounts to EspI from wild-type EPEC (Fig. 5A). This was despite a slight decrease in production of EspI$_{\Delta C7}$ in whole-cell lysates (Fig. 5A). As a control for bacterial lysis, we detected the same samples with antibodies to DnaK, which showed that the secreted protein fractions did not contain contaminating cytoplasmic proteins. We also examined the levels of EspI and EspI$_{\Delta C7}$ translocation into cells and found that both full-length and truncated EspI were translocated in similar amounts (Fig. 5B). Interestingly we observed two reactive bands for EspI and EspI$_{\Delta C7}$ in HeLa cells, suggesting that the protein may be processed by the host cell. At this stage, the reason for two bands corresponding to EspI is unknown. As a negative control, we constructed a *sepL* mutant of EPEC E2348/69, which secretes effectors but is unable to translocate proteins into the cell (Fig. 5B) (O'Connell *et al*., 2004; Deng *et al*., 2005). To characterize further the location of EspI and EspI$_{\Delta C7}$ in HeLa cells, we used confocal microscopy to take orthogonal sections through infected cells stained simultaneously for EspI or EspI$_{\Delta C7}$ and actin. Staining for both EspI and EspI$_{\Delta C7}$ clearly spanned the cell depth indicating that both proteins were located beneath the cell plasma membrane (Fig. 5C and D).

### *Colonization of mice by* C. rodentium espI *mutants*

Conservation of the C-terminal PDZ binding motif of EspI in *C. rodentium* suggested that EspI from *C. rodentium* would interact with the PDZ-domain proteins identified using EspI derived from EPEC. Therefore, the ability of *C. rodentium* EspI and EspI$_{\Delta C7}$ to interact with the six EspI Y2HS targets was tested. In contrast to EPEC EspI, TCOF1 interacted only weakly with EspI from *C. rodentium*, suggesting that TCOF1 is unlikely to be a target of EspI across all A/E pathogens (Fig. 6A). The remaining host cell proteins, on the other hand, exhibited equally strong interactions with EspI from *C. rodentium* that were dependent on the PDZ binding motif (Fig. 6A). This suggested that the functional role of the EspI PDZ binding motif could be studied *in vivo* using *C. rodentium* infection of mice.

To investigate the importance of the PDZ binding motif for virulence, the *C. rodentium* Δ*espI* mutant, ICC179, was complemented with full-length *espI$_{CR}$* and *espI$_{CR\Delta C7}$*. Derivatives of *C. rodentium* were used to inoculate C57BL/6 mice in single infections. Stool samples from mice infected with wild-type *C. rodentium* (pACYC184), ICC179 (pACYC184), ICC179 (pEspI$_{CR}$) or ICC179 (pEspI$_{CR\Delta C7}$) were collected daily up to 14 days post inoculation. The ability of the wild-type and mutant strains to colonize mice was monitored by performing viable counts on recovered stools. The stool counts of ICC179 (pEspI$_{CR\Delta C7}$) were comparable to the stool counts of wild-type *C. rodentium* (pACYC184) and ICC179 (pEspI$_{CR}$) over the course of the infection (Fig. 6B), indicating that the absence of the C-terminal PDZ binding motif of EspI did not lead to a colonization defect in single infections. In contrast, the stool counts for ICC179 (pACYC184) were approximately 100-fold lower at each time point compared with other *C. rodentium* strains (Fig. 6B). We also examined the degree of hyperplasia induced by derivatives of *C. rodentium* in C57BL/6 mice 10 days after inoculation, but found no significant differences in colon weight between wild-type infected mice and mice infected with ICC179 (pEspI$_{CR}$) or ICC179 (pEspI$_{CR\Delta C7}$) (Fig. 7). In addition, we examined colon sections by histology but found no significant differences in pathology and inflammation between groups of mice infected with wild-type *C. rodentium*, ICC179 (pEspI$_{CR}$) or ICC179 (pEspI$_{CR\Delta C7}$) (data not shown).

As a more subtle measure of virulence, we also investigated the ability of *C. rodentium* expressing full-length EspI$_{CR}$ to compete with *C. rodentium* expressing EspI$_{CR\Delta C7}$. Groups of C57BL/6 mice were inoculated in a ratio of 1:1 with a test strain and a reference strain of *C. rodentium* in

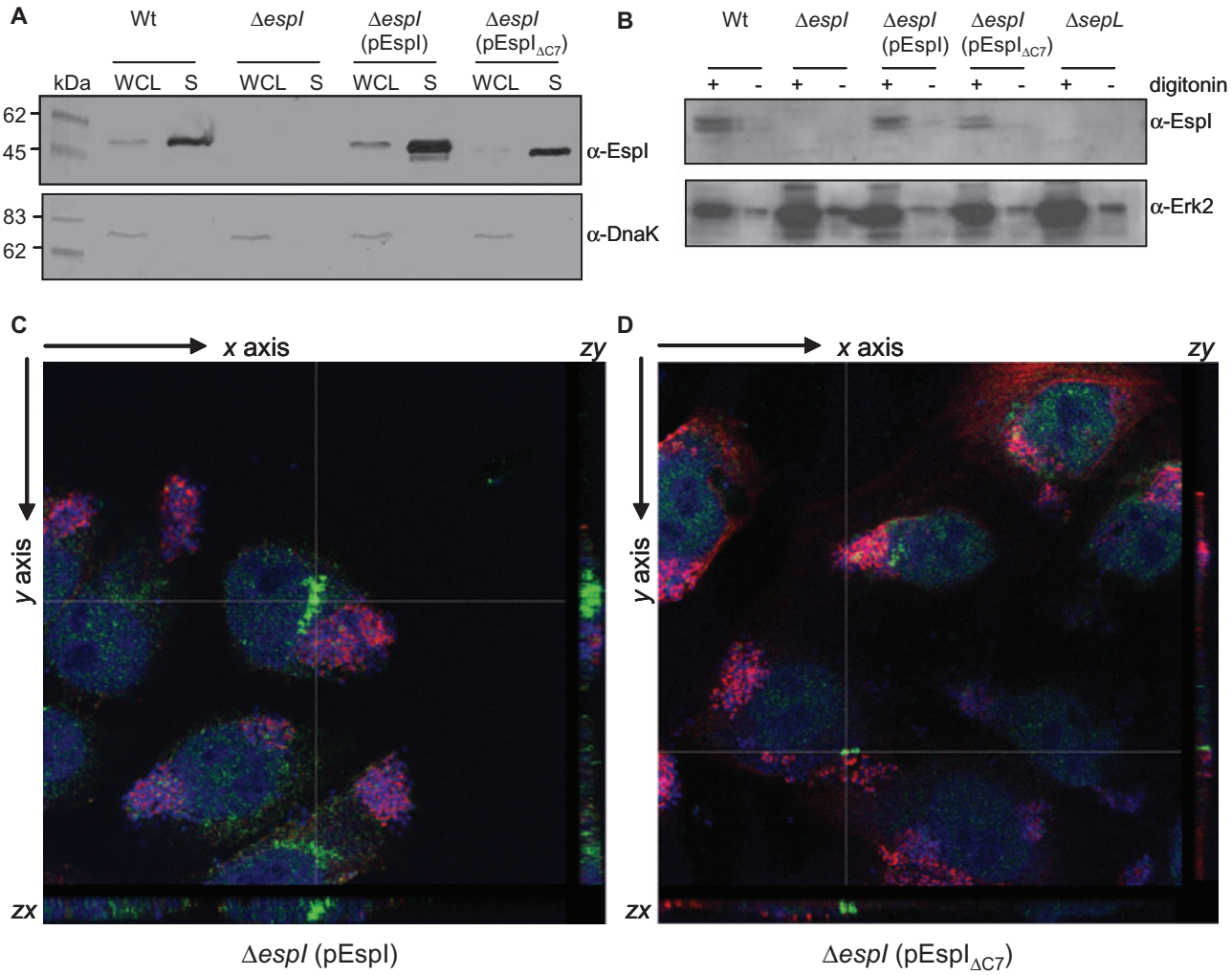


**Fig. 5.** A. Secretion of EspI and EspI$_{\Delta C7}$ by derivatives of EPEC E2348/69 grown in M9. EspI and the cytoplasmic protein DnaK were detected by immunoblot analysis of secreted proteins (S) and whole-cell lysates (WCL).
B. Translocation of EspI and EspI$_{\Delta C7}$ into HeLa cells infected with derivatives of EPEC E2348/69 was assessed as described previously (Aili *et al*., 2006). EspI and the HeLa cell cytoplasmic proteins, Erk1/2, were detected by immunoblot analysis of cell fractions. Translocated proteins should be present in the digitonin-treated HeLa cell fractions together with Erk1/2 and absent in the untreated preparations.
C and D. Confocal images of HeLa cells infected with Δ*espI* (pEspI) and Δ*espI* (pEspI$_{\Delta C7}$). Bars indicate where orthogonal sections of the image have been folded out to show depth of the cell (*zy* and *zx* sections), where the top of cell is at the edge of the field (right and bottom panels).

a mixed infection, and the competitive index (CI) was calculated 7 days after infection. The CI of ICC179 (test) in competition with wild-type *C. rodentium* (reference) was 0.000046 (Fig. 8), similar to the CI obtained in previous experiments (CI = 0.00005 in C3H/HeJ mice, 6 days post inoculation (Mundy *et al*., 2004a)). Upon transcomplementation with full-length EspI$_{CR}$, the CI of ICC179 (pEspI$_{CR}$) (test) in competition with wild-type *C. rodentium* (reference) was 1.77 (Fig. 8). This showed that carriage of full-length pEspI$_{CR}$ restored complete colonizing ability to the *Δespl* mutant. In contrast, the CI of ICC179 (pEspI$_{CR\Delta C7}$) (test) in competition with ICC179 (pEspI$_{CR}$) (reference) was 0.27, indicating that deletion of the last 7 amino acids from EspI resulted in a partial attenuation (Fig. 8). Therefore, the last 7 amino acids of EspI encompassing the PDZ binding motif offered an advantage to *C. rodentium in vivo* and modulated the virulence of *C. rodentium* in mixed infections. However, the entire deletion of *espI* had a much greater effect on virulence, indicating that EspI$_{CR\Delta C7}$ retained a major virulence function that was independent of the PDZ binding motif.

## Discussion

The T3SS effector, EspI, contributes to the virulence of *C. rodentium* in a mouse model of infection; however, the mechanism of action of EspI and its target(s) within the host cell remain largely uncharacterized. EspI localizes to

 

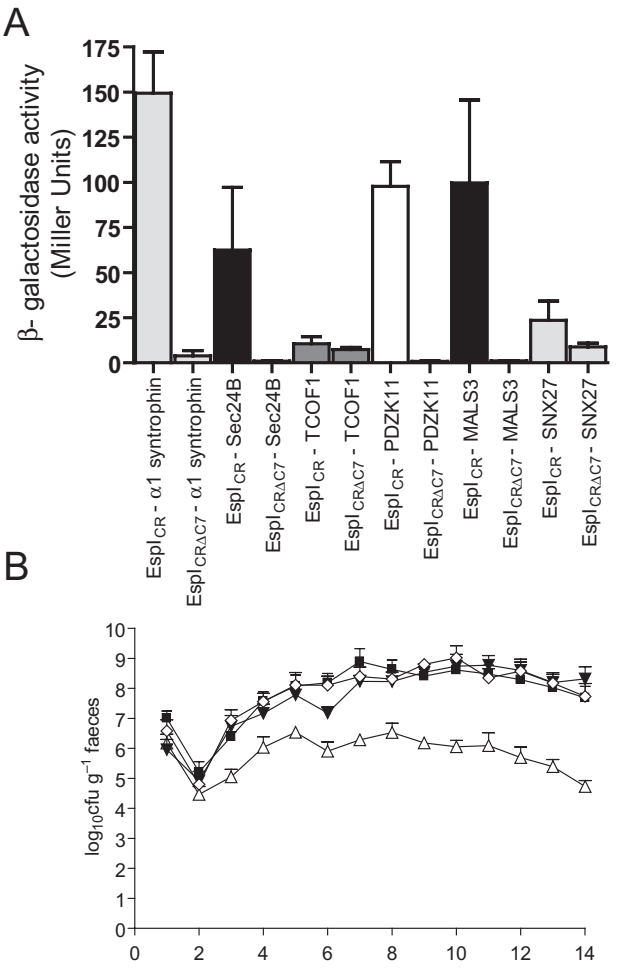


**Fig. 6.** A. Interaction of EspI$_{CR}$ and EspI$_{CRΔC7}$ from *C. rodentium* with α1 syntrophin, Sec24B, TCOF1, PDZK11, MALS3, SNX27 in the Y2HS. Interactions were analysed by assessing β-galactosidase activity in *S. cerevisiae* strains carrying EspI$_{CR}$ and EspI$_{CRΔC7}$ fusions to the binding domain of GAL4 and HeLa cDNA fusions to the activation domain of GAL4 as indicated.
B. Colonization of C57BL/6 mice with derivatives of *C. rodentium*. Groups of at least five 4- to 5-week-old male C57BL/6 mice were inoculated by oral gavage with *C. rodentium* wild-type ICC169 (■), ICC179 (pACYC184) (△), ICC179 (pEspI$_{CR}$) (▼), and ICC179 (pEspI$_{CRΔC7}$) (◇). Stool samples were collected daily up to 14 days post inoculation. Levels of gut colonization by *C. rodentium* were determined by plating serially diluted stool samples onto antibiotic selective media. Results are expressed as the mean log$_{10}$ cfu (± standard deviation) per gram stool for at least five animals.

Golgi apparatus upon translocation into infected host cells, although no classical Golgi-targeting motif is evident in the EspI amino acid sequence. Recently, Sec24B was identified as a binding partner of EspI in an independent study which also showed that EspI interfered with COPII vesicle formation (Kim *et al*., 2007). The consequences of this interaction for the virulence of A/E pathogens are unknown, but EspI may disrupt important protein secretion pathways in enterocytes that maintain the function and integrity of the intestinal epithelium.

In this study, we identified 15 putative eukaryotic binding partners of EspI using the Y2HS and PDZ-domain protein array overlaid with GST–EspI$_{50}$. Four of the six host cell proteins identified in the Y2HS contained PDZ domains. PDZ domains comprise six β-strands and two α-helices that form a large hydrophobic binding groove that specifically recognizes a C-terminal PDZ binding motif on target proteins (Harris and Lim, 2001). A multiple sequence alignment of known EspI proteins revealed a consensus class I PDZ binding motif present at the C-terminus of EspI. This was consistent with the possibility that EspI interacts specifically with a subset of PDZ-domain proteins. The PDZ-domain proteins identified in the Y2HS screen included syntrophin, MALS3, PDZK11 and SNX27, and additional PDZ-domain proteins identified from the protein array screen included MAGI-2 and MAGI-3, NHERF1 and NHERF2, PSD-95, SAP97, SAP102, PDZK1 and PDZK2. In addition, we identified two non-PDZ-domain proteins, Sec24B and TCOF1, in the Y2HS as putative binding partners of EspI.

Using the Y2HS, we found that the C-terminal 7 amino acids of EspI comprising the PDZ binding motif were necessary for EspI interactions with syntrophin, MALS3, PDZK11, SNX27 and Sec24B. Sec24B contains a Sec23/Sec24 helical domain and is a member of a protein complex of COPII vesicles that is responsible for the transport of proteins from the endoplasmic reticulum to the Golgi complex (Schekman and Orci, 1996). Even though Sec24B does not contain a PDZ domain, the interaction of EspI with Sec24B was dependent on the EspI PDZ binding motif.

The EPEC effector protein, Map, also has a PDZ binding motif that interacts with the host protein, NHERF1/EBP50 (Alto *et al*., 2006; Simpson *et al*., 2006). The class I PDZ binding motifs of EspI and Map, ETRV and DTRL, are very similar to each other apart from amino acid residues at positions −3 and 0. To examine the specificity of binding between EspI and putative eukaryotic binding partners, we tested the ability of a chimeric protein, EspI$_{DTRL}$, to interact with EspI targets. The interaction between EspI and α1 syntrophin, Sec24B, MALS3, PDZK11 but not TCOF1 or SNX27 was lost upon replacement of ETRV with the DTRL motif, emphasizing the importance of these residues to the specificity of interactions between native PDZ binding motifs and their targets (Harris and Lim, 2001). In addition, using the PDZ-domain array, we found that EspI interacted with the Map binding partner NHERF1 and that Map can bind α1 syntrophin in the Y2HS (data not shown). *In vivo*, the relevant interaction is likely to be dictated by protein location and tissue expression. For example, NHERF1 is highly expressed in the brush border of the intestinal epithelium (Ingraffea *et al*., 2002). The EspI interaction results presented here raise the possibility that both Map and EspI target NHERF1 during infection.

 

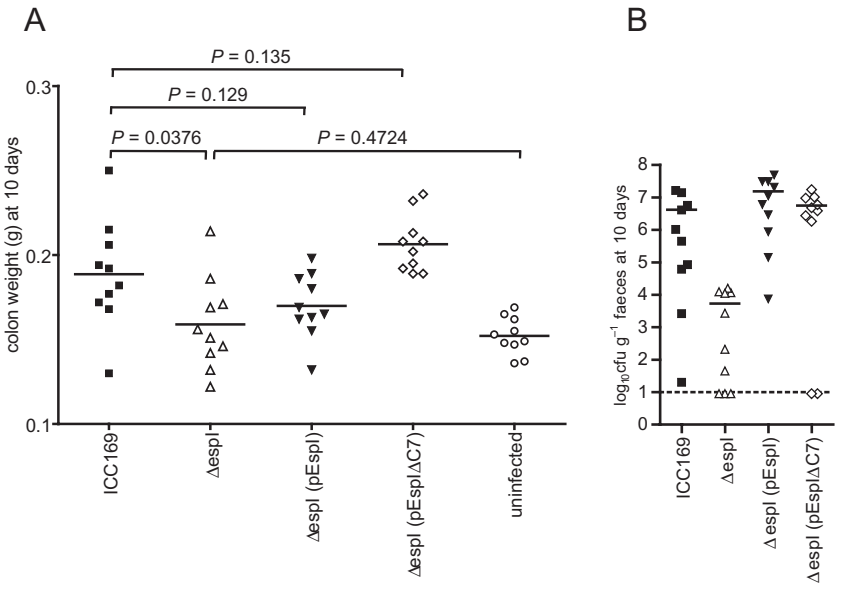


**Fig. 7.** Induction of colonic hyperplasia in C57BL/6 mice by derivatives of *C. rodentium*. A. Weight of colons dissected from C57BL/6 mice on day 10 post inoculation. Stools were removed from the dissected colon and remaining tissue was weighed. Data are shown as individual weights for each animal. B. Viable counts of *C. rodentium* recovered from faeces for individual C57BL/6 mice prior to dissection.

We found that deletion of the C-terminal 7 amino acids encompassing the EspI PDZ binding motif delayed EspI Golgi localization in HeLa cells. When translated into the *C. rodentium* infection model, the absence of the EspI PDZ binding motif resulted in reduced bacterial fitness *in vivo* compared with full-length EspI. This may reflect the reduced efficiency of Golgi targeting, which leads to reduced virulence when *C. rodentium* expressing $EspI_{\Delta C7}$ is in competition with *C. rodentium* expressing full-length EspI. Unfortunately, our repeated attempts to visualize EspI in frozen sections of colon taken from infected mice were unsuccessful and we were not able to confirm the trafficking results obtained *in vitro*. In single infections, *C. rodentium* expressing $EspI_{\Delta C7}$ showed similar levels of bacterial colonization and gut hyperplasia to *C. rodentium* expressing full-length EspI. This demonstrated that $EspI_{\Delta C7}$ retained a major virulence function and suggested that the truncated protein binds to other eukaryotic protein(s) in a PDZ binding motif-independent manner.

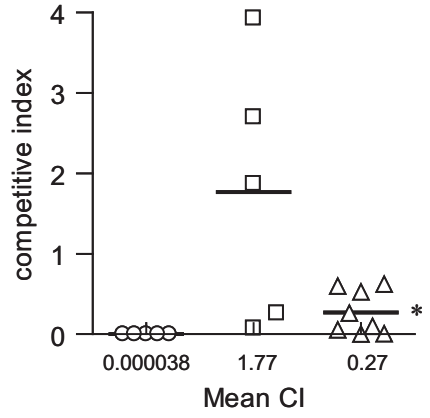


**Fig. 8.** Competitive index (CI) derived from the mixed-strain infections of C57BL/6 mice. Groups of at least five animals were inoculated by oral gavage with a 1:1 mixture of the Δ*espI* mutant, ICC179 (pACYC184) and wild-type *C. rodentium* ICC169 (pACYC184) (○), ICC179 ($pEspI_{CR}$) and ICC169 (pACYC184) (□), as well as ICC179 ($pEspICR_{\Delta C7}$) and ICC179 ($pEspI_{CR}$) (△). All mice were sacrificed 7 days post inoculation. The CI of the different *C. rodentium* strains in the initial inoculum and the mouse colon at the time of sacrifice was determined by plating serially diluted samples on agar plates containing selective antibiotics. The mean CI of each group is indicated on the graph by horizontal line. The mean CI of ICC179 (pACYC184) versus ICC169 (pACYC184) was 0.000046, ICC179 ($pEspI_{CR}$) versus ICC169 (pACYC184) was 1.77, and ICC179 ($pEspI_{CR\Delta C7}$) versus ICC179 ($pEspI_{CR}$) was 0.27. The asterisk indicates significantly less than ICC179 ($pEspI_{CR}$) versus ICC169 (pACYC184), $P = 0.0246$, unpaired two-tailed *t*-test.

Although in this study we sought to assess the contribution of the PDZ binding motif of EspI to Golgi trafficking and virulence rather than validate each of the 15 EspI targets identified, some of the putative PDZ-domain EspI binding partners nevertheless represent intriguing and novel targets in the eukaryotic cell. Syntrophin is a modular adaptor protein that comprises several interaction motifs, including PDZ and pleckstrin homology (PH) domains, and is important for maintaining membrane integrity and targeting signalling proteins and ion channels to the host cell membrane (Albrecht and Froehner, 2002). Several isoforms of syntrophin are found in mice and humans (α1, β1, β2, γ1 and γ2), and the expression of these isoforms differs among different tissue types (Adams *et al*., 1995; Ahn *et al*., 1996; Piluso *et al*., 2000). Using the PDZ-domain protein array, we found that EspI could bind four of the five isoforms of syntrophin. MALS3, also known as VELI-3 (Vertebrate LIN Seven 3), belongs to a family of mammalian homologues of *Caenorhabditis elegans* LIN-7 proteins that mediate basolateral targeting of epidermal growth factor receptor (Simske and Kim, 1995; Kaech *et al*., 1998). Depending on the type of mam-

 

**Table 3.** Bacterial and yeast strains used in this study.

| Strain or plasmid | Characteristic(s)[a] | Reference/source |
|---|---|---|
| Strain | | |
| *E. coli* | | |
| E2348/69 | Wild-type EPEC O127:H6 | Robins-Browne (1987) |
| EPEC Δ*espI* | E2348/69 Δ*espI* (Kan$^r$) | This study |
| EPEC Δ*sepL* | E2348/69 Δ*sepL* (Kan$^r$) | This study |
| BL21 (λDE3) | | |
| KC8 | *pyrF::Tn5, hsdR, leuB600, trpC9830, lacD74, strA, galK, hisB436* | Clontech |
| XL1-Blue | *recA1 endA1 gyrA96 thi-1 hsdR17 supE44 relA1 lac* [F′ *proAB lacIqZΔM15* Tn*10* (Tet$^r$)] | Stratagene |
| *C. rodentium* | | |
| ICC169 | *C. rodentium* wild-type strain ATCC 51459 (Nal$^r$) | Mundy *et al*. (2003) |
| ICC179 | ICC169 Δ*espI* (Nal$^r$Kan$^r$) | Mundy *et al*. (2004b) |
| *S. cerevisiae* | | |
| PJ69-4A | *MAT*a *trp1–901 leu2–3, 112 ura3–52 his3–200 gal4Δ gal80Δ LYS2::GAL1-HIS3 GAL2-ADE2 met2::Gal7-lacZ* | Clontech |
| Y187 | *MATa, trp 1–901, leu 2–3, 112, ura3–52, his3–200, gal4Δ, gal80Δ, LYS2:: GAL1$_{TATA}$ -HIS3, MEL1, GAL2$_{UAS}$ -GAL2$_{TATA}$ -ADE2, URA3:: MEL1$_{UAS}$ -MEL1$_{TATA}$ -lacZ* | Clontech |
| AH109 | *MATα*, *ura3–52, his3–200, ade 2–101, trp 1–901, leu 2–3, 112, gal4Δ, met–, gal80Δ, URA3::GAL1*$_{UAS}$ *-GAL1*$_{TATA}$*-lacZ, MEL1* | Clontech |
| Plasmid | | |
| pGBT9 | GAL4 DNA binding domain fusion protein expression vector (Amp$^r$) | Clontech |
| pGAD424 | GAL4 activation domain fusion protein expression vector (Amp$^r$) | Clontech |
| pGBTEspI | Derivative of pGBT9 encoding EspI from EPEC E2348/69 (Amp$^r$) | This study |
| pGBTEspI$_{\Delta C7}$ | Derivative of pGBT9 encoding EspI$_{\Delta C7}$ from EPEC E2348/69 (Amp$^r$) | This study |
| pGBTEspI$_{DTRL}$ | Derivative of pGBT9 encoding EspI$_{DTRL}$ (Amp$^r$) | This study |
| pGBTEspI$_{CR}$ | Derivative of pGBT9 encoding EspI from *C. rodentium* ICC169 (Amp$^r$) | This study |
| pGBTEspI$_{CR\Delta C7}$ | Derivative of pGBT9 encoding EspI$_{\Delta C7}$ from *C. rodentium* ICC169 (Amp$^r$) | This study |
| pGADT7-Rec-cDNA | Vector expressing GAL4 activation domain-HeLa protein fusion (Amp$^r$) | This study |
| pKD46 | Red recombinase helper plasmid (Amp$^r$) | Datsenko and Wanner (2000) |
| pKD4 | Red recombinase template plasmid (Kan$^r$) | Datsenko and Wanner (2000) |
| pACYC184 | Medium-copy number cloning vector (Cm$^r$ Tet$^r$) | New England Biolabs |
| pEspI | Derivative of pACYC184 encoding EspI from EPEC E2348/69 (Tet$^r$) | This study |
| pEspI$_{\Delta C7}$ | Derivative of pACYC184 encoding EspI$_{\Delta C7}$ from EPEC E2348/69 (Tet$^r$) | This study |
| pEspI$_{CR}$ | Derivative of pACYC184 encoding EspI from *C. rodentium* ICC169 (Tet$^r$) | This study |
| pEspI$_{CR\Delta C7}$ | Derivative of pACYC184 encoding EspI$_{\Delta C7}$ from *C. rodentium* ICC169 (Tet$^r$) | This study |
| pRSETEspI | Derivative of pRSETB encoding (His)$^6$EPEC EspI (Amp$^r$) | This study |
| pGEX3X | GST gene fusion vector (Amp$^r$) | Pharmacia Biotech |
| pGEX3XEspI$_{50}$ | pGEX3X encoding GST fused to the C-terminal 50 amino acids of EspI (Amp$^r$) | This study |

**a.** Kan, kanamycin; Nal, nalidixic acid; Tet, tetracycline; Cm, chloramphenicol; Amp, ampicillin.

malian cells under study, MALS proteins have various roles in the stabilization of MAGUK proteins (membrane-associated guanylate kinases) that are important for proper formation of tight junctions in epithelial cells (Straight *et al*., 2006). SNX27, also known as Mrt1, is a member of the sorting nexin family that is involved in endocytosis of plasma membrane receptors and trafficking of endocytic membrane (Worby and Dixon, 2002; Joubert *et al*., 2004). Interestingly, SNX9 was recently identified as a target of EspF, although no defect in clathrin-mediated endocytosis of transferrin was observed as a consequence of the EspF–SNX9 interaction (Marches *et al*., 2006). The function of PDZK11 is so far unknown (Strausberg *et al*., 2002).

In summary, our findings suggest that the C-terminal PDZ binding motif of EspI contributes to Golgi trafficking and modulates the function of the protein in virulence by interacting with a subset of host PDZ-domain proteins and Sec proteins. To characterize further the functional roles of EspI during A/E pathogenesis, it will be necessary to identify eukaryotic proteins that interact with EspI$_{\Delta C7}$ and to validate the PDZ-domain targets identified here as EspI binding partners in infected cells.

## Experimental procedures

### *Bacterial strains, yeast strains and growth conditions*

The bacterial strains, yeast strains and plasmids used in this study are listed in Table 3. Bacteria were grown at 30°C or 37°C in Luria–Bertani (LB) medium, Dulbecco's modified Eagle's medium (DMEM) or M9 supplemented with ampicillin (100 μg ml$^{-1}$), kanamycin (100 μg ml$^{-1}$), tetracycline (25 μg ml$^{-1}$), chloramphenicol (25 μg ml$^{-1}$) or nalidixic acid (50 μg ml$^{-1}$) when necessary. Yeast strains were grown at 30°C in YPD (yeast extract/peptone/dextrose) medium or yeast nitrogen minimal medium supplemented with 2% glucose and amino acids including histidine (20 μg ml$^{-1}$), methionine (20 μg ml$^{-1}$), tryptophan (20 μg ml$^{-1}$), adenine (20 μg ml$^{-1}$), uracil (20 μg ml$^{-1}$) and leucine (30 μg ml$^{-1}$) when necessary. For infection of HeLa cells, over-

**Table 4.** Oligonucleotide primers used in this study.

| Primer | Sequence (5′–3′) |
|---|---|
| EspIF787 | CGGAATTCATGAACATTCAACCGATCG |
| EspIR788 | CGGGATCCTTAGACTCTTGTTTCTTGG |
| EspIRΔ943 | CGGGATCCTTAATCAACGGTATCAACATAATTTGATGG |
| EspIF994 | CGGAATTCATGAACATTCAACCGAAC |
| EspIRΔ978 | CGGAATTCTTATTCAAAGGTGTCAACATAATTTGATG |
| EspIRDTRL | CGGGATCCCTACAGCCGAGTATCTTGGATTATATCAACGGTATC |
| rbsEspIF | CGGAATTCGATATTATTAATGGATATAAAC |
| EspIR945 | CGGAATTCTTAGACTCTTGTTTCTTGG |
| EspIRΔ958 | CGGAATTCTTAATCAACGGTATCAACATAATTTGATGG |
| ΔEspIF | ATGGATATAAACATGCAATAAGGATTTATCATGAACATTCAACCGATCGTTGTGTAGGCTGGAGCTGCTTC |
| ΔEspIR | CGTCATCCATTTCAGCTATTATTTTAAAATAAACAAGTTAAAGCTTAGACCATCTGAATATCCTCCTTA |
| Rec744 | CTATTCGATGATGAAGATACCCCACC |
| GSTEspIF | CGGGATCCCCATACGCGCAATGGAAGAAGG |
| ΔSepLF | GGTATTGAATTTAATCAAAACCCCGCATCTGTTTTTAATTCTAATTCATTAGATTTTGAAGTGTAGGCTGGAGCTGCTTC |
| ΔSepLR | CCTCCTTATAATCTATCACTTTACCAATCATTAATAATGTATTACTCCTCTGCTCGTTATCATATGAATATCCTCCTTAG |

night cultures of EPEC grown in DMEM were subcultured 1:10 into fresh DMEM with 2% fetal calf serum (FCS) supplemented with appropriate antibiotics and grown for 2 h with shaking at 37°C before being used to infect HeLa cell monolayers. The optical density ($A_{600}$) of the bacterial cultures was measured to standardize the inoculum before infection.

### *Construction of EspI expression vectors*

The primers used in this study are listed in Table 4. For use in the Y2HS, full-length *espI* and *espI*$_{\Delta C7}$ from EPEC E2348/69 were amplified using primer pairs EspIF787 and EspIR788 or EspIF787 and EspIRΔ943 respectively. The polymerase chain reaction (PCR) products were ligated into the EcoRI/BamHI sites of pGBT9 or pGAD424 to produce plasmids pGBTEspI and pGBTEspI$_{\Delta C7}$ (Table 3). The chimeric derivative, *espI*$_{DTRL}$, was amplified from EPEC E2348/69 using primers EspIF787 and EspIRDTRL to delete the ETRV motif of EPEC EspI but include the DRTL motif of Map (Table 4). The PCR products were ligated into the EcoRI/BamHI site of pGBT9 to produce pGBTEspI$_{DTRL}$ (Table 3). Full-length *espI* and *espI*$_{\Delta C7}$ were amplified from *C. rodentium* ICC169 using primers EspIF994 and EspIR788 or EspIF994 and EspIRΔ978 respectively (Table 4). The PCR products were cloned into EcoRI/BamHI or EcoRI sites of pGBT9 to produce plasmids pGBTEspI$_{CR}$ and pGBTEspI$_{CR\Delta C7}$ (Table 3).

For complementation of the *espI* mutants, full-length *espI* and *espI*$_{\Delta C7}$ including the putative ribosome binding sites were amplified from EPEC E2348/69 using primers rbsEspIF and EspIR945 or rbsEspIF and EspIRΔ958 respectively (Table 4). The PCR products were ligated into the EcoRI site of pACYC184 to produce plasmids, pEspI and pEspI$_{\Delta C7}$ (Table 3). Full-length *espI* and *espI*$_{\Delta C7}$ from *C. rodentium* including the putative ribosome binding site were amplified from *C. rodentium* ICC169 using primers rbsEspIF and EspIR945 or rbsEspIF and EspIRΔ978 (Table 4). The PCR products were cloned into EcoRI site of pACYC184 to produce plasmid pEspI$_{CR}$ and pEspI$_{CR\Delta C7}$ (Table 3).

For the construction of (His)$^6$-tagged EspI, full-length EPEC *espI* was amplified from EPEC E2348/69 using primers EspIF787 and EspIR945, and the digested PCR product was ligated into the EcoRI site of pRSETB to produce pRSETEspI (Table 3 and Table 4). pRSETEspI was transformed into *E. coli* BL21 (λDE3) for protein expression. The carboxyl-terminal 50 amino acids of EspI of EPEC E2348/69 were amplified using primers GSTEspIF and EspIR945 (Table 4). The PCR products were cloned into BamHI/EcoRI site of pGEX3X to produce plasmid pGEX3XEspI$_{50}$ (Table 3). pGEX3XEspI$_{50}$ was transformed into *E. coli* XL1-Blue for expression and purification of GST-fusion proteins for the screening of the PDZ-domain array.

### *Yeast two-hybrid HeLa cDNA library screen*

The BD Matchmaker pretransformed HeLa cDNA library (Clontech, Mountain View, CA, USA) was screened according to the manufacturer's protocols (Clontech PT3183-1 manual) to identify HeLa proteins interacting with EspI. The yeast strain AH109 (MATα) was transformed with pGBTEspI using the LiAc method and mated with Y187 (MATα) carrying the cDNA library in pGADT7 Rec plasmid. The mating mixtures were plated onto quadruple drop-out plates (Trp$^-$, Leu$^-$, Ade$^-$, His$^-$) to select for diploids expressing reporter genes. The pGADT7-Rec-cDNA plasmids were selectively rescued from those diploids with positive protein interactions into *E. coli* KC8. The pGADT7-Rec-cDNA plasmids were then sequenced using primer Rec744 to identify the cDNA inserts.

β-Galactosidase assays were performed according to the manufacturer's protocols (Clontech PT3024-1 manual). Briefly, the pGADT7-Rec-cDNA plasmid alone or with pGBTEspI (and also pGBT9, pGBTEspI$_{\Delta C7}$, pGBTEspI$_{DTRL}$, pGBTEspI$_{CR}$ or pGBTEspI$_{CR\Delta C7}$ when necessary) were transformed into *Saccharomyces cerevisiae* strain PJ69-4A using the LiAc method. Transformants were selected on Trp$^-$ Leu$^-$ plates and grown to an optical density ($A_{600}$) of 0.6 before lysis and assay for the level of β-galactosidase activity using ONPG as a substrate.

### *Screening of PDZ-domain array with GST–EspI$_{50}$*

Overnight cultures of *E. coli* XL1-Blue carrying pGEX3X or pGEX3XEspI$_{50}$ were diluted 1:100 into 400 ml of LB supplemented with appropriate antibiotics and grown to an optical density ($A_{600}$) of 0.5–0.8 at 30°C. Bacteria were pelleted by centrifugation, and the GST- or the GST–EspI$_{50}$ fusion proteins were purified using Scientifix™ GSH Agarose according to the manu-

 

facturer's protocols (Scientifix SGGSH11/04 manual). The eluted proteins were dialysed against $dH_2O$ overnight at 4°C to remove excess glutathione, and the concentration of the purified proteins was determined by Quick Start™ Bradford protein assay according to the manufacturer's protocols (Bio-rad).

To assess the binding of the GST–$EspI_{50}$ fusion protein to the PDZ-domain array, purified His-tagged PDZ-domain fusion proteins were spotted as previously described (Fam *et al.*, 2005; He *et al.*, 2006) at 1 μg per bin onto Nytran SuperCharge 96-grid nylon membranes (Schleicher and Schuell). The membranes were allowed to dry overnight and then blocked in 'blot buffer' (2% non-fat dry milk, 0.1% Tween-20, 50 mM NaCl, 10 mM Hepes, pH 7.4) for 30 min at room temperature. The arrays were then overlaid with either control GST- or GST–$EspI_{50}$ fusion protein (100 nM in blot buffer) overnight at 4°C. The overlaid arrays were washed three times for 5 min each with 20 ml blot buffer, incubated with anti-GST horseradish peroxidase-conjugated antibody (Amersham, 1:4000) for 1 h at room temperature, washed again three times for 5 min each with 20 ml blot buffer, and ultimately visualized via chemiluminescence with the ECL kit from Pierce.

### *Construction of EPEC E2348/69* espI *and* sepL *mutants*

The *espI* and *sepL* genes in EPEC E2348/69 were disrupted using the λ Red recombination system (Datsenko and Wanner, 2000). Briefly, the kanamycin-resistance gene was amplified from pKD4 by PCR using primers ΔEspIF and ΔEspIR or ΔSepLF and ΔSepLR. PCR products were *Dpn*1-digested before being electroporated into EPEC E2348/69 carrying the Red-recombinase expression plasmid, pKD46. Mutants were selected from LB plates supplemented with kanamycin and verified by PCR and sequencing for the replacement of *espI* or *sepL* with the kanamycin-resistance gene.

### *Generation of anti-EspI antiserum and immunofluorescence*

*Escherichia coli* BL21(λDE3) strain was transformed with pRSETEspI and grown to an optical density ($A_{600}$) of 0.4, after which it was induced with 0.4 mM IPTG for 4 h at 30°C. Bacteria were pelleted by centrifugation and lysed by a French pressure cell. $(His)^6$-EspI was purified using a $Ni^{2+}$-immobilized column according to the manufacturer's protocols (Qiagen, Hilden, Germany). Column-purified $(His)^6$-EspI was used to immunize a rabbit with ethically approved adjuvant performed by Chemicon (Temecula, CA, USA). The resulting antiserum was purified by absorption against the whole-cell lysates of M9-grown EPEC Δ*espI*. The specificity of the absorbed antiserum was tested by Western blotting of the EPEC wild-type and EPEC Δ*espI* whole-cell lysates.

For immunofluorescence, HeLa cells were grown to subconfluency on glass coverslips in 24-well tissue culture plates with DMEM containing 10% FCS and supplemented with 100 units $ml^{-1}$ penicillin and 0.1 mg $ml^{-1}$ streptomycin at 37°C in 5% $CO_2$. Prior to infection, HeLa cells were washed with prewarmed PBS before DMEM containing 5% FCS and 0.5% mannose with no antibiotics was added. EPEC derivatives were grown as described above and HeLa cells were infected at a multiplication of infection (moi) of approximately 10:1 for 5 h. For long incubations of live cells, after the initial 5 h infection period, EPEC derivatives were killed by the addition of penicillin and streptomycin, and incubated for up to 24 h before fixation and staining. Following infection (and, where indicated, prolonged incubation), HeLa cells were washed three times in PBS before being fixed in 1% paraformaldehyde in PBS for 20 min. Fixed cells were permeabilized in 0.1% Triton X-100 in PBS for 20 min prior to immunostaining. The primary antibodies used in this study, anti-EspI and mouse monoclonal anti-Golgin-97 CDF4 (Invitrogen, Carlsbad, CA, USA), were diluted 1/50 and 1/200 respectively in 0.2% BSA in PBS. Secondary antibodies, Alexa488-conjugated goat anti-rabbit antibodies (Invitrogen) and Alexa594-conjugated goat anti-mouse antibodies (Invitrogen), were both diluted 1/600 in 0.2% BSA in PBS. Permeabilized cells were incubated with primary antibodies for 1 h, washed three times in PBS, and then incubated with secondary antibodies for 1 h. For visualization of adherent bacteria and host cell nuclei, DAPI (Invitrogen) was diluted 1/10 000 in 0.2% BSA in PBS and applied to the cells for 5 min. Coverslips were mounted in DAKO fluorescent mounting medium (DAKO Corporation Carpinteria, USA) and stored at 4°C in the dark. Slides were examined under a 100× objective using an Olympus, BX51 microscope (Olympus, Tokyo, Japan). Images were acquired using an Olympus DP-70 digital camera and merged using DP controller software version 1.1.1.71. Alternatively for confocal microscopy, HeLa cells were infected with Δ*espI* (pEspI) or Δ*espI* ($pEspI_{\Delta C7}$) and stained simultaneously with anti-EspI antibodies as above and phalloidin-TRITC. In addition, bacterial and host cell nucleic acid was detected with Syto 61 (Invitrogen) and artificially coloured blue. Images were acquired using a Leica SP5 Multiphoton confocal microscope with the Leica Application Suite – Advanced Fluorescence (LAS AF) software version 1.6. Fluorescence samples were visualized with Argon 488 nm, HeNe 543 nm and HeNe 632 nm lasers using a 100× 1.4NA objective, and images were acquired at a resolution of 512 × 512 pixels, z sections taken at 120 nm step size, 12 bits (0–4095). Sequential acquisition of images occurred at PMT1495–540 nm and PMT2550–620 nm of cells infected with Δ*espI* (pEspI) 31 z-steps or Δ*espI* ($pEspI_{\Delta C7}$) 69 z-steps.

### *Preparation of secreted proteins*

Overnight cultures of EPEC grown in M9 were diluted 1:50 into 35 ml of M9 supplemented with appropriate antibiotics and grown with shaking to an optical density ($A_{600}$) of 1.0 at 37°C. The bacteria were pelleted by centrifugation, and the supernatant was filtered through 0.45 μm filter. Secreted proteins in the filtered supernatants were precipitated with 10% trichloroacetic acid (TCA) and washed twice in methanol. During the TCA precipitation and methanol wash steps, the secreted proteins were pelleted by centrifugation at 13 000 r.p.m., 4°C for 45 min. The protein pellet was dried at room temperature before being resuspended in 2× SDS loading buffer for SDS-PAGE and immunoblotting for EspI (1:500 dilution) and DnaK (Stressgen, 1:10 000 dilution).

### *Translocation of EspI and* $EspI_{\Delta C7}$

Effector translocation was assessed as described previously with minor modifications (Aili *et al.*, 2006). Briefly, HeLa cells were seeded at a density of $2 \times 10^6$ on 100 mm tissue culture dishes

 

approximately 40 h prior to infection. EPEC derivatives were grown as previously described, and HeLa cells were infected at an moi of approximately 1000:1 for 4 h. Two dishes were used for each strain, one for lysis with digitonin and the other to act as an unlysed control. After the infection period, the HeLa cells were washed five times with PBS before the addition of 1 ml proteinase K (250 μg $ml^{-1}$) in order to remove extracellular proteins. The proteinase K solution was removed after being evenly distributed on the dishes which were incubated at room temperature for 20 min. In total, 0.5 ml of PMSF (6 mM) was added to stop the proteinase K enzymatic reaction, and infected cells were scraped off the dishes and collected in microfuge tubes. In total, 200 μl of 2% digitonin was added to lyse the infected cells, and unbroken cells were slowly passaged through a 22-gauge needle using a syringe (approximately 6 times) for complete lysis. A total of 200 μl of PBS was added to the unlysed-control tube. Bacteria, unbroken HeLa cells and ruptured HeLa cells' debris were pelleted by centrifugation at 5000 r.p.m. for 5 min, and the supernatants were subjected to SDS-PAGE and immunoblotting for EspI (1:500 dilution) and Erk1/2 (BD Biosciences, 1:5000 dilution).

### *Infection of mice with derivatives of* C. rodentium

In mixed-infection competition experiments, bacterial test strains were grown to stationary phase in LB broth containing appropriate antibiotics. Overnight cultures of the bacterial strains were pelleted by centrifugation and resuspended in PBS. The two bacterial strains to be compared were combined in a ratio of 1:1 (approximately $2 \times 10^9$ cfu for each strain) in 200 μl PBS and used to infect 4- to 5-week-old male C57BL/6 mice by oral gavage. Dilutions of the inoculum were plated on respective antibiotic-containing plates to determine the ratio of the two bacterial strains (test strain/reference strain) in the inoculum. Seven days after inoculation, mice were killed by $CO_2$ inhalation, and bacteria were recovered by plating dilutions of homogenized colon onto respective antibiotic plates to determine the ratio of test strain cfu to reference strain cfu in the intestine. The CI was calculated by dividing the ratio of test strain cfu and reference strain cfu recovered from the colon by the ratio of test strain cfu to reference strain cfu in the inoculum (Mundy *et al*., 2003). A test strain with a CI of $< 0.5$ was considered to be attenuated, whereas a CI $\geq 1$ indicated that the test strain colonized at least as well as the reference strain. The CI was analysed using five or more animals per group and assessed for significance using an unpaired Student's two-tailed *t*-test.

In single-infection experiments, bacterial strains were pelleted by centrifugation and resuspended in PBS. At least four 4- to 5-week-old male C57BL/6 mice were inoculated by oral gavage with approximately $2 \times 10^9$ cfu in 200 μl PBS. The viable count of the inoculum was determined retrospectively by plating dilutions of the inoculum on plates with and without relevant antibiotics. Stool samples were collected daily up to 14 days after infection. The viable count per gram of stool was determined by plating serial dilutions of stool samples onto antibiotic selective media. Single-infection results were expressed as the mean $\log_{10}$cfu per gram feces from at least five animals for each bacterial strain. Hyperplasia was assessed 10 days after infection, whereupon mice were killed, and the distal section of colon from the cecum to the rectum was aseptically removed and weighed after the removal of fecal pellets and cecal contents. A 1 cm section of colon was removed for fixation in 10% formalin and sectioning for haematoxylin and eosin histology, and subsequent assessment of gut pathology and inflammation. The remaining organ was homogenized mechanically in 5 ml of sterile PBS using a Seward 80 stomacher, and the number of viable bacteria per gram of organ homogenate was determined by plating onto LB agar containing the appropriate antibiotics.

## Acknowledgements

We are grateful to Danni Krmek for her expert assistance with *C. rodentium* infections, and to Stephen Firth from the Monash MicroImaging Facility for help with confocal microscopy. We are also indebted to Margareta Aili for advice on translocation assays, to Vicki Bennett-Wood for her help with haematoxylin and eosin sections, and to Dorit Becher for her advice and help with EspI staining of mouse frozen tissue sections. This work was supported by grants from the Australian Research Council and the Australian National Health and Medical Research Council. S.F.L. is the recipient of a Monash Graduate Scholarship and a Monash International Postgraduate Research Scholarship. R.A.H. is supported by grants from the National Institutes of Health and W. M. Keck Foundation.

## References

Adams, M.E., Dwyer, T.M., Dowler, L.L., White, R.A., and Froehner, S.C. (1995) Mouse alpha 1- and beta 2-syntrophin gene structure, chromosome localization, and homology with a discs large domain. *J Biol Chem* **270:** 25859–25865.

Ahn, A.H., Freener, C.A., Gussoni, E., Yoshida, M., Ozawa, E., and Kunkel, L.M. (1996) The three human syntrophin genes are expressed in diverse tissues, have distinct chromosomal locations, and each bind to dystrophin and its relatives. *J Biol Chem* **271:** 2724–2730.

Aili, M., Isaksson, E.L., Hallberg, B., Wolf-Watz, H., and Rosqvist, R. (2006) Functional analysis of the YopE GTPase-activating protein (GAP) activity of *Yersinia pseudotuberculosis*. *Cell Microbiol* **8:** 1020–1033.

Albrecht, D.E., and Froehner, S.C. (2002) Syntrophins and dystrobrevins: defining the dystrophin scaffold at synapses. *Neurosignals* **11:** 123–129.

Alto, N.M., Shao, F., Lazar, C.S., Brost, R.L., Chua, G., Mattoo, S., *et al*. (2006) Identification of a bacterial type III effector family with G protein mimicry functions. *Cell* **124:** 133–145.

Batchelor, M., Prasannan, S., Daniell, S., Reece, S., Connerton, I., Bloomberg, G., *et al*. (2000) Structural basis for recognition of the translocated intimin receptor (Tir) by intimin from enteropathogenic *Escherichia coli*. *EMBO J* **19:** 2452–2464.

Batchelor, M., Guignot, J., Patel, A., Cummings, N., Cleary, J., Knutton, S., *et al*. (2004) Involvement of the intermediate filament protein cytokeratin-18 in actin pedestal formation during EPEC infection. *EMBO Rep* **5:** 219.

Creuzburg, K., Recktenwald, J., Kuhle, V., Herold, S., Hensel, M., and Schmidt, H. (2005) The Shiga toxin 1-converting bacteriophage BP-4795 encodes an NleA-like type III effector protein. *J Bacteriol* **187:** 8494–8498.

Datsenko, K.A., and Wanner, B.L. (2000) One-step inactiva-

 

tion of chromosomal genes in *Escherichia coli* K-12 using PCR products. *Proc Natl Acad Sci USA* **97:** 6640–6645.

Deng, W., Li, Y., Hardwidge, P.R., Frey, E.A., Pfuetzner, R.A., Lee, S., *et al.* (2005) Regulation of type III secretion hierarchy of translocators and effectors in attaching and effacing bacterial pathogens. *Infect Immun* **73:** 2135–2146.

Elliott, S.J., Wainwright, L.A., McDaniel, T.K., Jarvis, K.G., Deng, Y.K., Lai, L.C., *et al.* (1998) The complete sequence of the locus of enterocyte effacement (LEE) from enteropathogenic *Escherichia coli* E2348/69. *Mol Microbiol* **28:** 1–4.

Fam, S.R., Paquet, M., Castleberry, A.M., Oller, H., Lee, C.J., Traynelis, S.F., *et al.* (2005) P2Y1 receptor signaling is controlled by interaction with the PDZ scaffold NHERF-2. *Proc Natl Acad Sci USA* **102:** 8042–8047.

Garmendia, J., Frankel, G., and Crepin, V.F. (2005) Enteropathogenic and enterohemorrhagic *Escherichia coli* infections: translocation, translocation, translocation. *Infect Immun* **73:** 2573–2585.

Goosney, D.L., DeVinney, R., Pfuetzner, R.A., Frey, E.A., Strynadka, N.C., and Finlay, B.B. (2000) Enteropathogenic *E. coli* translocated intimin receptor, Tir, interacts directly with alpha-actinin. *Curr Biol* **10:** 735–738.

Gruenheid, S., DeVinney, R., Bladt, F., Goosney, D., Gelkop, S., Gish, G.D., *et al.* (2001) Enteropathogenic *E. coli* Tir binds Nck to initiate actin pedestal formation in host cells. *Nat Cell Biol* **3:** 856–859.

Gruenheid, S., Sekirov, I., Thomas, N.A., Deng, W., O'Donnell, P., Goode, D., *et al.* (2004) Identification and characterization of NleA, a non-LEE-encoded type III translocated virulence factor of enterohaemorrhagic *Escherichia coli* O157: H7. *Mol Microbiol* **51:** 1233–1249.

Harris, B.Z., and Lim, W.A. (2001) Mechanism and role of PDZ domains in signaling complex assembly. *J Cell Sci* **114:** 3219–3231.

Hartland, E.L., Batchelor, M., Delahay, R.M., Hale, C., Matthews, S., Dougan, G., *et al.* (1999) Binding of intimin from enteropathogenic *Escherichia coli* to Tir and to host cells. *Mol Microbiol* **32:** 151–158.

He, J., Bellini, M., Inuzuka, H., Xu, J., Xiong, Y., Yang, X., *et al.* (2006) Proteomic analysis of beta1–adrenergic receptor interactions with PDZ scaffold proteins. *J Biol Chem* **281:** 2820–2827.

Ingraffea, J., Reczek, D., and Bretscher, A. (2002) Distinct cell type-specific expression of scaffolding proteins EBP50 and E3KARP: EBP50 is generally expressed with ezrin in specific epithelia, whereas E3KARP is not. *Eur J Cell Biol* **81:** 61–68.

Jarvis, K.G., and Kaper, J.B. (1996) Secretion of extracellular proteins by enterohemorrhagic *Escherichia coli* via a putative type III secretion system. *Infect Immun* **64:** 4826–4829.

Jelen, F., Oleksy, A., Smietana, K., and Otlewski, J. (2003) PDZ domains – common players in the cell signaling. *Acta Biochim Pol* **50:** 985–1017.

Jerse, A.E., Yu, J., Tall, B.D. and Kaper, J.B. (1990) A genetic locus of enteropathogenic *Escherichia coli* necessary for the production of attaching and effacing lesions on tissue culture cell. *Proc Natl Acad Sci USA* **87:** 7839–7843.

Joubert, L., Hanson, B., Barthet, G., Sebben, M., Claeysen, S., Hong, W., *et al.* (2004) New sorting nexin (SNX27) and NHERF specifically interact with the 5-HT4a receptor splice variant: roles in receptor targeting. *J Cell Sci* **117:** 5367–5379.

Kaech, S.M., Whitfield, C.W., and Kim, S.K. (1998) The LIN-2/LIN-7/LIN-10 complex mediates basolateral membrane localization of the *C. elegans* EGF receptor LET-23 in vulval epithelial cells. *Cell* **94:** 761–771.

Kelly, M., Hart, E., Mundy, R., Marches, O., Wiles, S., Badea, L., *et al.* (2006) Essential role of the type III secretion system effector NleB in colonization of mice by *Citrobacter rodentium*. *Infect Immun* **74:** 2328–2337.

Kenny, B. (1999) Phosphorylation of tyrosine 474 of the enteropathogenic *Escherichia coli* (EPEC) Tir receptor molecule is essential for actin nucleating activity and is preceded by additional host modifications. *Mol Microbiol* **31:** 1229–1241.

Kenny, B., DeVinney, R., Stein, M., Reinscheid, D.J., Frey, E.A., and Finlay, B.B. (1997) Enteropathogenic *E. coli* (EPEC) transfers its receptor for intimate adherence into mammalian cells. *Cell* **91:** 511–520.

Kim, J., Thanabalasuriar, A., Chaworth-Musters, T., Fromme, J.C., Frey, E.A., Lario, P.I., *et al.* (2007) The bacterial virulence factor NleA binds and disrupts function of mammalian COPII. *Cell Host Microbe* **2:** 160–171.

Lim, I.A., Hall, D.D., and Hell, J.W. (2002) Selectivity and promiscuity of the first and second PDZ domains of PSD-95 and synapse-associated protein 102. *J Biol Chem* **277:** 21697–21711.

Luo, Y., Frey, E.A., Pfuetzner, R.A., Creagh, A.L., Knoechel, D.G., Haynes, C.A., *et al.* (2000) Crystal structure of enteropathogenic *Escherichia coli* intimin-receptor complex. *Nature* **405:** 1073–1077.

Marches, O., Batchelor, M., Shaw, R.K., Patel, A., Cummings, N., Nagai, T., *et al.* (2006) EspF of enteropathogenic *Escherichia coli* binds sorting nexin 9. *J Bacteriol* **188:** 3110–3115.

Mundy, R., Pickard, D., Wilson, R.K., Simmons, C.P., Dougan, G., and Frankel, G. (2003) Identification of a novel type IV pilus gene cluster required for gastrointestinal colonization of *Citrobacter rodentium*. *Mol Microbiol* **48:** 795–809.

Mundy, R., Petrovska, L., Smollett, K., Simpson, N., Wilson, R.K., Yu, J., *et al.* (2004a) Identification of a novel *Citrobacter rodentium* type III secreted protein, EspI, and roles of this and other secreted proteins in infection. *Infect Immun* **72:** 2288–2302.

Mundy, R., and Jenkins, C., Yu, J., Smith, H., and Frankel, G. (2004b) Distribution of espI among clinical enterohaemorrhagic and enteropathogenic *Escherichia coli* isolates. *J Med Microbiol* **53:** 1145–1149.

Mundy, R., MacDonald, T.T., Dougan, G., Frankel, G., and Wiles, S. (2005) *Citrobacter rodentium* of mice and man. *Cell Microbiol* **7:** 1697–1706.

O'Connell, C.B., Creasey, E.A., Knutton, S., Elliott, S., Crowther, L.J., Luo, W., *et al.* (2004) SepL, a protein required for enteropathogenic *Escherichia coli* type III translocation, interacts with secretion component SepD. *Mol Microbiol* **52:** 1613–1625.

Piluso, G., Mirabella, M., Ricci, E., Belsito, A., Abbondanza, C., Servidei, S., *et al.* (2000) Gamma1- and gamma2-

syntrophins, two novel dystrophin-binding proteins localized in neuronal cells. *J Biol Chem* **275:** 15851–15860.

Piserchio, A., Spaller, M., and Mierke, D.F. (2006) Targeting the PDZ domains of molecular scaffolds of transmembrane ion channels. *Aaps J* **8:** E396–E401.

Robins-Browne, R.M. (1987) Traditional enteropathogenic *Escherichia coli* of infantile diarrhea. *Rev Infect Dis* **9:** 28–53.

Schauer, D.B., and Falkow, S. (1993) Attaching and effacing locus of a *Citrobacter freundii* biotype that causes transmissible murine colonic hyperplasia. *Infect Immun* **61:** 2486–2492.

Schekman, R., and Orci, L. (1996) Coat proteins and vesicle budding. *Science* **271:** 1526–1533.

Simpson, N., Shaw, R., Crepin, V.F., Mundy, R., FitzGerald, A.J., Cummings, N., *et al.* (2006) The enteropathogenic *Escherichia coli* type III secretion system effector Map binds EBP50/NHERF1: implication for cell signalling and diarrhoea. *Mol Microbiol* **60:** 349–363.

Simske, J.S., and Kim, S.K. (1995) Sequential signalling during *Caenorhabditis elegans* vulval induction. *Nature* **375:** 142–146.

Songyang, Z., Fanning, A.S., Fu, C., Xu, J., Marfatia, S.M., Chishti, A.H., *et al.* (1997) Recognition of unique carboxyl-terminal motifs by distinct PDZ domains. *Science* **275:** 73–77.

Straight, S.W., Pieczynski, J.N., Whiteman, E.L., Liu, C.J., and Margolis, B. (2006) Mammalian lin-7 stabilizes polarity protein complexes. *J Biol Chem* **281:** 37738–37747.

Strausberg, R.L., Feingold, E.A., Grouse, L.H., Derge, J.G., Klausner, R.D., Collins, F.S., *et al.* (2002) Generation and initial analysis of more than 15,000 full-length human and mouse cDNA sequences. *Proc Natl Acad Sci USA* **99:** 16899–16903.

Tobe, T., Beatson, S.A., Taniguchi, H., Abe, H., Bailey, C.M., Fivian, A., *et al.* (2006) An extensive repertoire of type III secretion effectors in *Escherichia coli* O157 and the role of lambdoid phages in their dissemination. *Proc Natl Acad Sci USA* **103:** 14941–14946.

Worby, C.A., and Dixon, J.E. (2002) Sorting out the cellular functions of sorting nexins. *Nat Rev Mol Cell Biol* **3:** 919–931.

Zhang, Y., Yeh, S., Appleton, B.A., Held, H.A., Kausalya, P.J., Phua, D.C., *et al.* (2006) Convergent and divergent ligand specificity among PDZ domains of the LAP and zonula occludens (ZO) families. *J Biol Chem* **281:** 22299–22311.

 